Computer simulation of mining in faulted ground

by S. L. CROUCH*, Ph.D. (Minnesota) (Visitor)

SYNOPSIS

This paper describes a numerical procedure for the computation of the displacements and stresses induced by the mining of a tabular ore deposit in faulted ground. The numerical procedure is based on the displacement discontinuity method, which can be regarded as an application of Salamon's 'face element principle' to cases in which the reef plane is faulted into several sections, or even folded in an arbitrary way. An element of a fault is modelled in the same manner as an element of the reef, except that a fault element is allowed to undergo permanent inelastic deformation (i.e., slip) if the stresses transmitted through the fault-filling material satisfy a Mohr–Coulomb yield condition.

An iterative technique for the incorporation of a Mohr–Coulomb yield condition in the general displacement discontinuity method is explained. This technique is illustrated by means of a simple example involving the mining of a flat-lying reef intersected by a fault. The displacements and stresses at selected locations along the fault are examined as the reef is mined, element by element. A consideration of the energy changes reveals that the occurrence of slip along a fault leads to a sudden increase in the energy release rate due to mining as the excavation intersects the fault. The energy release rate then falls off abruptly to a value less than that which would occur in the absence of any slip, and gradually builds up to re-establish the conditions that would exist in unfaulted ground.

SAMEVATTING

Hierdie referaat beskryf 'n numeriese prosedure vir die berekening van die verplasings en spannings veroorsaak deur die ontginning van 'n tafelvormige ertsafsetting in grond waar verskuiwings plaasgevind het. Die numeriese prosedure word gebaseer op die verplasingsdiskontinuïteitmetode wat beskou kan word as 'n toepassing van Salamon se "frontelementbeginsel" op gevalle waar die rifvlak in verskillende seksies verskuif of selfs op 'n willekeurige wyse gevou is. 'n Element van 'n verskuiwing word op dieselfde wyse as 'n element van die rif gemodelleer, behalwe dat 'n verskuiwingselement toegelaat word om permanente vervorming (d.w.s. glip) te ondergaan as die spannings wat oorgebring word deur die materiaal wat die verskuiwing vul, aan 'n Mohr–Coulomb-swigtingsvoorwaarde voldoen.

'n Herhalingstegniek vir die insluiting van 'n Mohr–Coulomb-swigtingsvoorwaarde by die algemene verplasingsdiskontinuïteitmetode word verduidelik. Hierdie tegniek word geïllustreer deur middel van 'n eenvoudige voorbeeld wat die ontginning behels van 'n plat rif wat deur 'n verskuiwing gekruis word. Die verplasings en spannings word op sekere uitgesoekte plekke langs die verskuiwing element vir element ondersoek soos die rif ontgin word. 'n Beskouing van die energieveranderinge toon dat die voorkoms van glip langs 'n verskuiwing lei tot 'n skielike toename in die energievrystellingstempo as gevolg van die mynbou wanneer die uitgrawing die verskuiwing kruis. Die energievrystellingstempo neem dan skielik af tot 'n kleiner waarde as wat in die afwesigheid van enige glip sal voorkom en bou dan geleidelik op om die toestande te herstel wat daar sou bestaan het in grond waarin daar geen verskuiwings plaasgevind het nie.

Introduction

Rock mechanics problems associated with the mining of tabular ore deposits are well known to South African mining engineers. Current practice in the planning of excavations in such deposits requires an estimate of the displacements and stresses induced by mining. Based upon principles set forth by Salamon[1–3], both analogue and digital computer techniques have been developed for this purpose (see, for example, Salamon[4]). The digital techniques are typified by a suite of computer programs used routinely in South Africa and known as the MINSIM programs.

During the time that the MINSIM programs were being developed in South Africa[5, 6], a parallel line of research was being pursued at the University of Minnesota[7, 8]. The latter work ultimately led to a somewhat more general numerical procedure called the displacement discontinuity method[9, 10]. This method can be regarded as an application of Salamon's face element principle to cases in which the reef plane is faulted into several sections, or even folded in an arbitrary way.

A particularly useful feature of the displacement discontinuity method is that it can be used to model *geologic discontinuities* (e.g., joints or faults) in the vicinity of an excavation. It is possible, for example, to model the opening or closing of a joint or the slipping of a fault as an excavation is enlarged. The purpose of this paper is to explain how this can be accomplished and to illustrate the use of the displacement discontinuity method for a particular problem involving the mining of a reef that intersects a fault. For simplicity, we shall restrict our attention to problems that can be treated in two dimensions. All the ideas given here can be extended to three dimensions, but this has not yet been done.

*Department of Civil and Mineral Engineering, University of Minnesota, Minneapolis, U.S.A.

Displacement Discontinuity Method

The displacement discontinuity method is based on the analytical solution to the problem of a constant displacement discontinuity, or dislocation, over a finite line segment in an infinite elastic body. The numerical procedure consists of the placing of a certain number, say N, of elemental displacement discontinuities along the boundaries of the region to be analysed, and then setting up and solving a system of algebraic equations to find the discontinuity values that produce prescribed displacements or stresses at the boundaries. This procedure is applicable to general cavity-type problems[9], but is explained most easily for the case when the boundaries in question are thin slits, or cracks, in an elastic solid.

Fig. 1 (a) illustrates the particular case of a single curved crack in an otherwise continuous body. It is assumed that the crack can be represented with sufficient accuracy by N straight-line segments joined end to end. The positions and orientations of these segments are

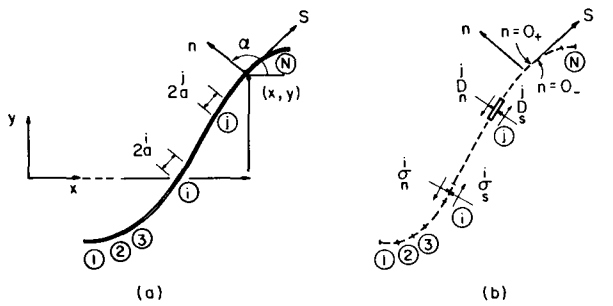

Fig. 1—Representation of a crack by N elemental displacement discontinuities

specified with reference to a Cartesian coordinate system, the x,y system shown in the figure. If the surfaces of the crack are subjected to stress (for example, a uniform fluid pressure p), they will displace relative to one another. In other words, the displacements will be *discontinuous* across the crack. The displacement discontinuity method is a means of finding a discrete approximation to the smooth distribution of displacement discontinuity that occurs in reality. This discrete approximation is found with reference to the N subdivisions of the crack depicted in Fig. 1 (a). Each of these subdivisions will be referred to as an *elemental displacement discontinuity*.

The elemental displacement discontinuities are defined with respect to the local coordinates s and n indicated in Fig. 1. These coordinates are respectively parallel and perpendicular to the crack; they therefore vary from point to point along the crack. Fig. 1 (b) depicts a single elemental displacement discontinuity at the j-th segment of the crack. The *normal* component of displacement discontinuity at this segment is called $\underset{n}{D}$; the tangential, or shear, component is called $\underset{s}{D}$. These quantities are defined in terms of the normal and shear displacements on the two sides of the crack as follows:

$$\underset{s}{D}=\underset{s}{u}^{-}-\underset{s}{u}^{+} \quad , \quad \underset{n}{D}=\underset{n}{u}^{-}-\underset{n}{u}^{+} \qquad \ldots\ldots\ldots \quad (1)$$

In these definitions, $\underset{s}{u}$ and $\underset{n}{u}$ refer to the shear (s) and normal (n) displacements of the j-th segment of the crack. The superscripts + and − denote respectively the *positive and negative surfaces of the crack*. The positive surface is the one that is encountered as the crack is approached from a point in the solid through positive values of n (i.e., $n\rightarrow 0_+$). The negative surface is defined similarly for the case that the crack is approached through negative values of n (i.e., $n\rightarrow 0_-$).

The local displacements $\underset{s}{u}$ and $\underset{n}{u}$ form the two components of a vector. They are positive in the positive directions of s and n in Fig. 1, irrespective of whether we are considering the positive or the negative side of the crack. As a consequence, it follows from equation (1) that the normal component of displacement discontinuity $\underset{n}{D}$ is positive if the two surfaces of the crack displace toward one another. Similarly, the component $\underset{s}{D}$ is positive if the positive surface of the crack moves to the left with respect to the negative surface, cf. Fig. 1 (b).

The analytical solution is available for the case of a constant displacement discontinuity D_s, D_n over an arbitrarily oriented, finite line segment in an infinite (or a semi-infinite) elastic body. This solution can be used to compute the displacements and stresses anywhere in the body in terms of the values of the displacement discontinuity components D_s and D_n. In particular, the shear and normal stresses at the midpoint of the i-th segment in Fig. 1 (b) can be expressed in terms of the displacement discontinuity components at the j-th segment as follows[10]:

$$\begin{aligned}\underset{s}{\sigma}&=\underset{ss}{A}\,\underset{s}{D}+\underset{sn}{A}\,\underset{n}{D}\\ &\qquad\qquad\qquad\qquad\qquad\qquad\qquad\qquad (2)\\ \underset{n}{\sigma}&=\underset{ns}{A}\,\underset{s}{D}+\underset{nn}{A}\,\underset{n}{D}\end{aligned}$$

The quantities $\underset{ss}{A}$, etc. in these equations are called *influence coefficients*. The coefficient $\underset{ns}{A}$, for example, gives the normal stress at the i-th segment ($\underset{n}{\sigma}$) in terms of the shear component of displacement discontinuity at the j-th segment ($\underset{s}{D}$). The stress component $\underset{n}{\sigma}$ is taken positive for compression; the component $\underset{s}{\sigma}$ is positive if it acts to the left with respect to the outward normal to the line in question. These quantities are shown in the positive sense in Fig. 1 (b).

Explicit expressions could be written for the influence coefficients $\underset{ss}{A}$, etc. in equations (2). These are too complicated to merit quotation here, however, and the interested reader is referred to the work mentioned earlier[9, 10] for details. Suffice it to say that the influence coefficients depend upon the elastic constants of the material and the position and orientation of the i-th segment with respect to the j-th segment. The coefficients are always finite. If we consider the case that i equals j, equations (2) give the shear and normal stresses at the midpoint of the j-th segment, i.e., the segment that has discontinuous displacements, by construction. The stresses $\underset{s}{\sigma}$ and $\underset{n}{\sigma}$ are finite, and represent the minimum values of the shear and normal stresses over the j-th segment*. We shall consider these stresses as being representative of those occurring over the entire segment.

Returning now to the crack problem depicted in Fig. 1 (a), we place an elemental displacement discontinuity at each of the N segments and write, from equations (2),

*The stresses theoretically are infinite at the endpoints of the segment. We avoid these singularities by agreeing only to consider the stresses at the midpoint.

$$\left.\begin{aligned} \overset{i}{\sigma}_{s} &= \sum_{j=1}^{N} \overset{ij}{A}_{ss}\,\overset{j}{D}_{s} + \sum_{j=1}^{N} \overset{ij}{A}_{sn}\,\overset{j}{D}_{n} \\ \overset{i}{\sigma}_{n} &= \sum_{j=1}^{N} \overset{ij}{A}_{ns}\,\overset{j}{D}_{s} + \sum_{j=1}^{N} \overset{ij}{A}_{nn}\,\overset{j}{D}_{n} \end{aligned}\right\} \quad i=1 \text{ to } N \quad \ldots\ldots \quad (3)$$

This result follows from the principle of superposition, which is valid because the N elemental displacement discontinuities are independent entities. If we specify the values of the stresses $\overset{i}{\sigma}_{s}$ and $\overset{i}{\sigma}_{n}$ for i=1 to N, then equations (3) are a system of $2N$ simultaneous linear equations in $2N$ unknowns: the displacement discontinuity components $\overset{i}{D}_{s}$ and $\overset{i}{D}_{n}$ for i=1 to N. These equations can be solved by standard methods of numerical analysis, e.g., elimination or iteration.

Once the elemental displacement discontinuity components have been found for a particular problem, we can compute the displacements and stresses at any point in the body by summing the effects of the individual elemental discontinuities. The displacements along the crack of Fig. 1 (a), for instance, are given by expressions of the form

$$\left.\begin{aligned} \overset{i}{u}{}^{\pm}_{s} &= \sum_{j=1}^{N} \overset{ij}{B}{}^{\pm}_{ss}\,\overset{j}{D}_{s} + \sum_{j=1}^{N} \overset{ij}{B}{}^{\pm}_{sn}\,\overset{j}{D}_{n} \\ \overset{i}{u}{}^{\pm}_{n} &= \sum_{j=1}^{N} \overset{ij}{B}{}^{\pm}_{ns}\,\overset{j}{D}_{s} + \sum_{j=1}^{N} \overset{ij}{B}{}^{\pm}_{nn}\,\overset{j}{D}_{n} \end{aligned}\right\} \quad i=1 \text{ to } N \quad \ldots\ldots \quad (4)$$

where $\overset{ij}{B}{}^{\pm}_{ss}$, etc. are influence coefficients for the boundary displacements. The displacements $\overset{i}{u}_{s}$ and $\overset{i}{u}_{n}$ are discontinuous when passing from one side of the i-th segment to the other, so we must distinguish between these two sides when computing the influence coefficients in equations (4). The symbol $\pm$ is used to call attention to this fact. Expressions for coefficients $\overset{ij}{B}{}^{\pm}_{ss}$, etc. are recorded elsewhere[9, 10].

Mining Applications for Seam or Reef Deposits

An important class of mining problems involves excavations in seam or reef-type deposits. Such deposits have the characteristic that they are very thin in one dimension and fairly extensive in the other two. If the seam and the excavations in it are uniform in one direction, say along strike, then a two-dimensional (plane strain) analysis can be adopted. We shall suppose that this is the case.

The displacement discontinuity method is ideally suited to the analysis of displacements and stresses induced by the mining of seam or reeftype deposits. Each elemental displacement discontinuity can be regarded, for example, as an element of the seam or reef. The values of the displacement discontinuity components D_{n} and D_{s} in this context are known respectively as the *closure* and the *ride* (Salamon[1])*. We shall refer to the elemental displacement discontinuities as *seam elements*, which are comparable to the *face elements* introduced by Salamon[1]. We adopt the present terminology to distinguish seam elements from *fault elements*, which are discussed later in this paper.

In analysing the displacements and stresses due to the mining of a seam deposit, we formulate the problem in terms of induced stresses. We accomplish this by imagining that the excavation boundaries are subjected to the *negatives* of the pre-existing normal and shear stresses. We compute in this way the displacement and stress changes due to the excavations. The complete solution then is given by the sum of the displacement and stress changes (which are zero at infinity) and the original conditions, taking the original displacements to be zero everywhere. This guarantees that the resultant, or total, stresses will be zero across any mined seam element, unless the closure and ride of the element are impeded in some way (as, for example, by a no-overlap or 'complete closure' restriction).

If we imagine that the curved crack depicted in Fig. 1 (a) represents a folded seam, then we may consider that each of the N line segments in the figure is a seam element. Some of the elements could be mined, and some unmined. In either case, the *induced stresses* $\overset{i}{\sigma}_{s}$ and $\overset{i}{\sigma}_{n}$ are given by equations (3), where $\overset{j}{D}_{s}$ and $\overset{j}{D}_{n}$ for j=1 to N are the ride and closure components, respectively. We can develop a system of algebraic equations for determining the closure and ride components from equations (3) by considering the boundary conditions at each seam element, i=1 to N.

First, if the i-th element is mined, the *total* stresses at the element must be zero, provided the two surfaces of the element do not come into contact. Denoting the pre-existing, or primitive, shear and normal stresses at the i-th element by $(\overset{i}{\sigma}_{s})_{0}$ and $(\overset{i}{\sigma}_{n})_{0}$, respectively, we can express this condition as follows:

$$\left.\begin{aligned} (\overset{i}{\sigma}_{s})_{\text{total}} &= \overset{i}{\sigma}_{s} + (\overset{i}{\sigma}_{s})_{0} = 0 \\ (\overset{i}{\sigma}_{n})_{\text{total}} &= \overset{i}{\sigma}_{n} + (\overset{i}{\sigma}_{n})_{0} = 0 \end{aligned}\right\} \quad \overset{i}{D}_{n} < h_{0}, \quad \ldots\ldots\ldots \quad (5)$$

where h_{0} is the thickness of the element. The constraint $\overset{i}{D}_{n} < h_{0}$ specifies that the two surfaces of the excavation do not come into contact at the i-th element. If this constraint were not met, it would mean that the two surfaces of the element overlap, which is physically impossible†.

*Salamon actually used the term *convergence* to denote what is referred to in this paper as closure, i.e., D_{n}. The term *closure* is adopted here to avoid confusion later when it becomes necessary to speak about the convergence of a sequence of numerical approximations.

†If the surfaces of the excavation do come into contact at the i-th element, then the total stresses at the element will not be zero. In order to calculate the values of these stresses, we replace equations (5) with conditions that the closure be *equal* to the seam thickness and that the ride be equal to the value that it had just at the moment of contact.

Another type of boundary condition applies if the i-th element is unmined. In this case, the normal and shear stresses induced at the element will cause it to deform. We approximate this deformation by saying that the induced stresses are related to the closure and ride as follows:

$$\begin{aligned} \overset{i}{\sigma}_{s} &= G_{seam} \overset{i}{D}_{s}/h_0 = K_s \overset{i}{D}_{s} \\ \overset{i}{\sigma}_{n} &= E_{seam} \overset{i}{D}_{n}/h_0 = K_n \overset{i}{D}_{n}, \end{aligned} \quad \ldots\ldots\ldots\ldots (6)$$

where E_{seam} and G_{seam} are the Young's modulus and the shear modulus of the seam material. These conditions are equivalent to saying that the surfaces of the element are connected by a spring that has a constant normal stiffness K_n and a constant shear stiffness K_s.

The combination of equations (3) and (5) or equations (3) and (6) specifies the i-th ones of a system of algebraic equations for determining the closure and ride components at all elements along the seam. If the i-th element is mined, equations (3) and (5) yield

$$\left.\begin{aligned} -\overset{i}{(\sigma)}_{s0} &= \sum_{j=1}^{N} \overset{ij}{A}_{ss} \overset{j}{D}_{s} + \sum_{j=1}^{N} \overset{ij}{A}_{sn} \overset{j}{D}_{n} \\ -\overset{i}{(\sigma)}_{n0} &= \sum_{j=1}^{N} \overset{ij}{A}_{ns} \overset{j}{D}_{s} + \sum_{j=1}^{N} \overset{ij}{A}_{nn} \overset{j}{D}_{n} \end{aligned}\right\} \overset{i}{D}_{n} < h_0 \quad \ldots\ldots (7)$$

If the i-th element is unmined, equations (3) and (6) give

$$\begin{aligned} 0 &= -K_s \overset{i}{D}_{s} + \sum_{j=1}^{N} \overset{ij}{A}_{ss} \overset{j}{D}_{s} + \sum_{j=1}^{N} \overset{ij}{A}_{sn} \overset{j}{D}_{n} \\ 0 &= -K_n \overset{i}{D}_{n} + \sum_{j=1}^{N} \overset{ij}{A}_{ns} \overset{j}{D}_{s} + \sum_{j=1}^{N} \overset{ij}{A}_{nn} \overset{j}{D}_{n} \end{aligned} \quad \ldots\ldots\ldots (8)$$

Since either equations (7) or equations (8) will apply at each element, i.e., for i=1 to N, these equations constitute a system of $2N$ algebraic equations in $2N$ unknowns. After solving them, we can compute the displacements and stresses at any point in the body in terms of $\overset{i}{D}_{s}$ and $\overset{i}{D}_{n}$ for i=1 to N.

Simulation of Mining

In reality, an underground excavation is produced in a series of stages, or steps. A slightly different boundary configuration is involved at each stage. We shall refer to the process of modelling the step-by-step creation of an underground excavation as *simulation of mining*.

Simulation of mining is especially simple for a seam or reef-type deposit. In this case, we simulate the extraction of the seam, step by step, simply by changing the boundary conditions at the appropriate elements. For example, in order to mine a particular element along the seam, we change the boundary conditions from equations (6) to equations (5). It is necessary, of course, to solve a new problem at each step of the simulation. If, however, we are solving the system of equations by iteration, then the solution for one step will serve as a very good approximation for the next step, and the required results can be found fairly quickly.

Computation of Energy Release Rates

Simulation of mining is necessary for any problem that involves a nonlinear phenomenon, because such a phenomenon must be modelled by an incremental process. We shall discuss two important examples of this below: complete closure of a mined seam element, and slip along a fault. First, however, we note that, as an added benefit of the simulation procedure, we can calculate directly the energy release rate due to mining[4].

The energy release rate due to the mining of a single element is given by the following expression:

$$\Delta U = \tfrac{1}{2}\left[\overset{i}{(\sigma)}'_{s\,total} \overset{i}{D}_{s} + \overset{i}{(\sigma)}'_{n\,total} \overset{i}{D}_{n}\right], \quad \ldots\ldots\ldots (9)$$

where $\overset{i}{(\sigma)}'_{s\,total}$ and $\overset{i}{(\sigma)}'_{n\,total}$ are the total shear and normal stresses that existed at the i-th element just prior to the mining of that element; $\overset{i}{D}_{s}$ and $\overset{i}{D}_{n}$ are the ride and closure experienced by the same element after it has been mined. The energy release rate represents a *spatial rate*, it has units[4] of joules per square metre (J/m^2).

If more than one element is mined at a particular mining step, the energy release rate is given by a simple sum of terms as in equation (9), divided by the number of elements mined at that step.

Complete Closure

The boundary conditions considered above for a mined seam element specifically excluded the possibility of the surfaces of the excavation coming into contact at the element in question. This situation is referred to as complete closure. Since a condition of complete closure can occur in reality, it is necessary to include this possibility in the boundary conditions for a mined seam element.

A complete closure condition is, in principle, fairly easy to incorporate in a mining problem. The most natural way of accomplishing this is to simulate the creation of an excavation, element by element, restricting the closure at any element to *no more* than the seam thickness, h_0. In other words, if at some stage of computation the closure at a particular element is just equal to the seam thickness, then we require it to remain at that value for all the subsequent stages. In addition, we require the ride component at the element to remain at the value that it has when the complete closure condition occurs. The boundary conditions for a mined seam element that undergoes complete closure can therefore be written as

$$\overset{i}{D}_{n} = h_0 \quad , \quad \overset{i}{D}_{s} = \overset{i}{D}^{*}_{s}, \quad \ldots\ldots\ldots\ldots (10)$$

where $\overset{i}{D}^{*}_{s}$ is the ride that exists at the i-th element for the stage of mining at which the closure of this element is just equal to the seam thickness.

In practice, the above procedure cannot be followed directly because it will seldom happen that the closure of an element becomes *just* equal to the seam thickness

at a particular stage of mining. Usually, a small amount of *overlap* initially will be indicated as a consequence of modelling the mining process in discrete steps. This overlap, which cannot occur in reality, might be indicated at several elements simultaneously. One cannot infer from this, however, that complete closure has actually occurred at all of these elements. In order to see this, we might imagine a case in which an overlap is indicated at three elements, side by side. If we suppose that only the centre element undergoes complete closure and then we re-analyse the problem with this constraint, we may find that the closures of the other two elements now are less than the seam thickness. These two elements therefore do not experience complete closure because they are 'propped open' when the closure is limited at the centre element.

In a general problem, it is desirable to have a systematic way of determining which elements actually undergo complete closure at a certain stage of mining. We can construct a particularly effective procedure by using the notion of successive approximations in combination with an iterative solution for the system of algebraic equations. This procedure, which can be viewed as a means of enforcing the constraints represented by equations (10) during the process of iteration, is summarized as follows.

(1) We begin with a certain stage of mining at which complete closure is imminent at one or more elements. The system of equations at this stage is represented by equations (7) for all the mined elements and equations (8) for all the unmined elements.

(2) At each cycle of iteration, we shall obtain trial values for the closure and ride at all the elements. These values are denoted as $\underset{n}{\overset{i}{D}}^{(k)}$ and $\underset{s}{\overset{i}{D}}^{(k)}$ for the k-th approximations of the closure and ride at the i-th element.

(3) If the i-th element is mined, we test the value of the k-th approximation of the closure to see whether it is greater than or equal to the seam thickness. If it is, we assume that the solution for this element is given by $\underset{n}{\overset{i}{D}}=h_0$ and $\underset{s}{\overset{i}{D}}=\underset{s}{\overset{i}{D}}^{(k)}$. In other words, we replace equations (7) by equations (10) as the i-th ones of the system of algebraic equations, with $\underset{s}{\overset{i}{D}}^{*}=\underset{s}{\overset{i}{D}}^{(k)}$.

(4) At the next cycle of iteration, we compute the stresses acting across all the elements that were assumed to undergo complete closure at the previous cycle. The normal stress across any such element must be compressive*. If a tensile stress is indicated, we conclude that the element has not, in fact, undergone complete closure and we return to equations (7) for the next cycle of iteration.

(5) Continuing in this way, we obtain a solution that satisfies equations (7) at all the mined elements that are not completely closed, equations (8) at all the unmined elements, and equations (10) at all the mined elements that are completely closed. The normal stress across all the latter elements will be compressive.

(6) We then simulate the next mining step and repeat the entire procedure.

In using this approach, it is important that the separate mining steps should be small enough to allow the zone of complete closure to develop as gradually as possible. This is because the ride at a completely closed element is required to remain at the value that it had just as the element became completely closed. Unlike the closure, we are not able to set a limit on the amount of ride that can occur. As a consequence, we have no criterion for modifying the value of the constrained ride $\underset{s}{\overset{i}{D}}^{*}$ used in the successive approximations approach. However, if the mining steps are taken small enough, the zone of complete closure will develop in a gradual way and the constrained values of the ride will not be subject to serious error.

*In the absence of any externally applied forces, a tensile stress cannot be developed normal to the surfaces of an excavation.

Mohr–Coulomb Slip Condition

In the analysis of mining problems, it is often necessary to model the effects of major structural features, such as faults, in the rock. For computational purposes, a fault can be represented in much the same way as a seam; that is, it can be thought of as a 'crack' with a compressible filling. The filling material will have associated with it a certain normal stiffness and a certain shear stiffness, which in part govern the amount of relative movement between the fault surfaces. A realistic representation of a fault, however, should include a constraint between the normal and shear stresses that can be transmitted through the filling material. Such a constraint for a typical element i can be written from the familiar Mohr–Coulomb condition as

$$\pm\left[(\overset{i}{\underset{s}{\sigma}})_{\text{total}}\right]_{\text{yield}}=c+(\overset{i}{\underset{n}{\sigma}})_{\text{total}}\tan\phi, \quad \ldots\ldots\ldots (11)$$

where c and ϕ respectively are the cohesion and the angle of friction of the fault-filling material.

A seam or fault element that is subject to the constraint expressed by equation (11) will be called a *Mohr–Coulomb element*. A Mohr–Coulomb element behaves exactly as an ordinary seam element, except that the total shear stress across it cannot exceed the value specified by equation (11). Fulfilment of this condition at a particular element requires that the element should be allowed to undergo a certain amount of inelastic deformation, or permanent slip, in the transverse direction. We shall discuss next how the magnitude and direction of the permanent slip can be computed.

Suppose that, at a certain stage of mining, the normal and shear stresses and the closure and ride at the i-th Mohr–Coulomb element have been computed. If condition (11) is not met at this stage of mining, and if it has not been met at any previous stage, then the total shear stress, $(\overset{i}{\underset{s}{\sigma}})_{\text{total}}$, and the ride, $\underset{s}{\overset{i}{D}}$, will lie at some point, say A, on the initial, linear portion of the curve for shear stress against ride shown in Fig. 2. The origin,

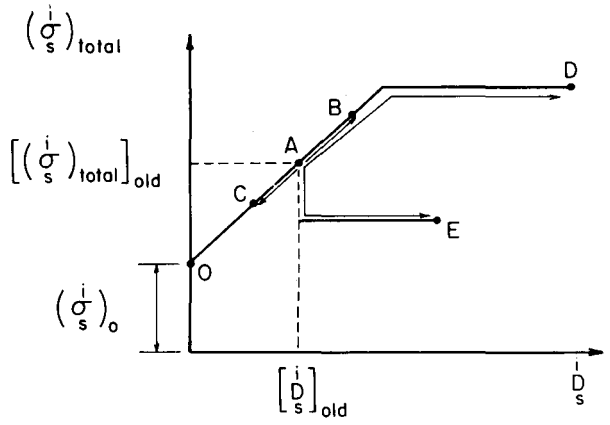

Fig. 2—Total shear stress–ride relationships of a Mohr–Coulomb element

point 0, of this curve represents the conditions that existed at the i-th element before any mining took place; the initial shear stress is $(\sigma)_{s\ 0}^{i}$ and the initial ride is zero.

At the next stage of mining, the i-th element may load or unload elastically, or it may fail in accordance with equation (11). The cases of elastic loading and unloading are indicated in Fig. 2 by points B and C, respectively. Two cases of failure, or slip, are indicated in the figure by points D and E. Point D corresponds to failure for a total *normal stress* that is greater than or equal to the value that occurred at the element at the previous stage of mining. Point E corresponds to failure for a reduced normal stress.

The particular path that will be followed from point A in Fig. 2 depends upon the value of the total normal stress, $(\sigma)_{n\ total}^{i}$. This stress is defined as the sum of the primitive normal stress, $(\sigma)_{n\ 0}^{i}$, and the induced normal stress, σ_{n}^{i}, i.e.,

$$(\sigma)_{n\ total}^{i}=(\sigma)_{n\ 0}^{i}+\sigma_{n}^{i} \quad \ldots\ldots\ldots\ldots\ldots\ldots (12)$$

or, using equation (3),

$$(\sigma)_{n\ total}^{i}=(\sigma)_{n\ 0}^{i}+\sum_{j=1}^{N} A_{ns}^{ij} D_{s}^{j}+\sum_{j=1}^{N} A_{nn}^{ij} D_{n}^{j} \quad \ldots\ldots (13)$$

Similarly, the total shear stress at the i-th element is given by the relation

$$(\sigma)_{s\ total}^{i}=(\sigma)_{s\ 0}^{i}+\sum_{j=1}^{N} A_{ss}^{ij} D_{s}^{j}+\sum_{j=1}^{N} A_{sn}^{ij} D_{n}^{j} \quad (14)$$

If the magnitude of this stress is less than the value of the yield stress as computed from equations (11) and (12), then the element will load or unload elastically in shear. In this case, the total shear stress will be equal to the value of the shear stress from the previous stage of mining,

$[(\sigma)_{s\ total}^{i}]_{old}$, plus an increment, $\Delta(\sigma)_{s\ total}^{i}$:

$$(\sigma)_{s\ total}^{i}=[(\sigma)_{s\ total}^{i}]_{old}+\Delta(\sigma)_{s\ total}^{i} \quad \ldots\ldots\ldots (15)$$

Since the element behaves in a linearly elastic manner, we can express the increment in shear stress in terms of the *change* in the ride as follows:

$$\Delta(\sigma)_{s\ total}^{i}=K_{s}\left[D_{s}^{i}-(D)_{s\ old}^{i}\right], \quad \ldots\ldots\ldots (16)$$

cf. equations (6). Equations (14) to (16) can now be combined to give

$$\left[(\sigma)_{s\ total}^{i}\right]_{old}-K_{s}(D)_{s\ old}^{i}-(\sigma)_{s\ 0}^{i}=-K_{s}D_{s}^{i}+\sum_{j=1}^{N} A_{ss}^{ij} D_{s}^{j}+$$

$$\sum_{j=1}^{N} A_{sn}^{ij} D_{n}^{j} \quad \ldots\ldots\ldots\ldots\ldots\ldots (17)$$

This expression can be regarded as an equation for the computation of D_{s}^{i} for the case when yield condition (11) is not met. It should be noted that the left-hand side of equation (17) is zero if the element has not previously experienced any slip. A Mohr–Coulomb element in this case is equivalent to an unmined seam element under the action of a shear stress, and equation (17) is exactly the same as the first of equations (8).

The magnitude of the shear stress $(\sigma)_{s\ total}^{i}$ from equation (14) cannot exceed the value of the yield stress $[(\sigma)_{s\ total}^{i}]_{yield}$ from equation (11). Therefore, if the element is yielding, the shear stress must *equal* the yield stress. Equations (11) and (14) give in this case

$$\pm\left[(\sigma)_{s\ total}^{i}\right]_{yield}-(\sigma)_{s\ 0}^{i}=\sum_{j=1}^{N} A_{ss}^{ij} D_{s}^{j}+\sum_{j=1}^{N} A_{sn}^{ij} D_{n}^{j}, \quad \ldots (18)$$

which can be regarded as an equation for the computation of D_{s}^{i}. The positive value of the yield stress $[(\sigma)_{s\ total}^{i}]_{yield}$ is used if the shear stress $(\sigma)_{s\ total}^{i}$ is positive, and the negative value is used if it is negative.

Equations (17) and (18) are the governing equations for the ride at the i-th Mohr–Coulomb element for any particular stage of mining. The corresponding equation for the closure D_{n}^{i} is given by the second of equations (8), i.e.,

$$0=-K_{n}D_{n}^{i}+\sum_{j=1}^{N} A_{ns}^{ij} D_{s}^{j}+\sum_{j=1}^{N} A_{nn}^{ij} D_{n}^{j} \quad \ldots\ldots\ldots (19)$$

Equations (17) or (18) and (19) can be satisfied for each Mohr–Coulomb element by an iterative process analogous to that described previously for complete closure of a mined seam element. This process is summarized as follows.

(1) At any stage of mining, a system of $2N$ equations in $2N$ unknowns will have to be solved. Each equation will relate to a particular type of element, for example, a seam element (either mined or unmined) or a Mohr–Coulomb element.

(2) At each cycle of iteration we shall obtain trial values for the closure and ride at each element. These values can be denoted by $\overset{i\,(k)}{D}_{n}$ and $\overset{i\,(k)}{D}_{s}$ for the k-th estimates of the closure and ride, respectively, at the i-th element. Trial values of the normal and shear stresses are found from equations (13) and (14). The trial stresses can be denoted by $(\overset{i\,(k)}{\sigma})_{n\,\text{total}}$ and $(\overset{i\,(k)}{\sigma})_{s\,\text{total}}$.

(3) If the i-th element is a Mohr–Coulomb element, we must check to see whether or not yield condition (11) is met. Since the total normal stress is not known precisely at this stage of iteration, we compute a 'trial yield stress' $\left[(\overset{i}{\sigma})_{s\,\text{total}}\right]^{(k)}_{\text{yield}}$ as follows:

$$\left[(\overset{i}{\sigma})_{s\,\text{total}}\right]^{(k)}_{\text{yield}} = c + (\overset{i}{\sigma})^{(k)}_{n\,\text{total}} \tan\phi \quad \ldots\ldots\ldots \quad (20)$$

(4) If, in terms of the trial values of the stresses, the yield condition *is not met*, we use equations (19) and (17) to compute the next approximations of the closure and ride at the i-th element.

(5) If, in terms of the trial values of the stresses, the yield condition *is met*, we use equations (19) and (18) to compute the next approximations of the closure and ride at the i-th element.

(6) Continuing in this way, we arrive at a solution that satisfies equations (17) or (18) and (19) at each Mohr–Coulomb element and meets the appropriate boundary conditions for all the other types of elements.

(7) We then simulate the next stage of mining and repeat the entire procedure.

The iterative procedure explained above allows a Mohr–Coulomb element to pass freely from an elastic state to a yielded one, and *vice versa*. This 'reversal of status' might occur between any two stages of mining, or it might occur between any two cycles of iteration. Neither of these situations presents any particular difficulties, although the latter can cause the rate of convergence of the overall iteration process to be somewhat slow in certain cases.

'Cracked' Mohr–Coulomb Element

In the discussion so far it has been tacitly assumed that the yield stress $\left[(\overset{i}{\sigma})_{s\,\text{total}}\right]_{\text{yield}}$ computed from equation (11) is positive. This will be the case provided $(\overset{i}{\sigma})_{n\,\text{total}}$ is greater than $-c$ cotan ϕ, as can be seen from Fig. 3. The two inclined, straight lines in the figure are the Mohr–Coulomb envelope lines; all possible combinations of normal and shear stress must lie on or be within these lines.

The iterative procedure explained above must be modified to include the case for which the yield stress computed from equation (11) is negative. This is accomplished by allowing the element to 'crack open' in the event that $(\sigma)_{n\,\text{total}}$ is less than $-c$ cotan ϕ. The boundary conditions for such an element are that the total normal and shear stresses are zero. A 'cracked' Mohr–Coulomb element is therefore equivalent to a mined seam element, and equations (7) must be satisfied for each such element.

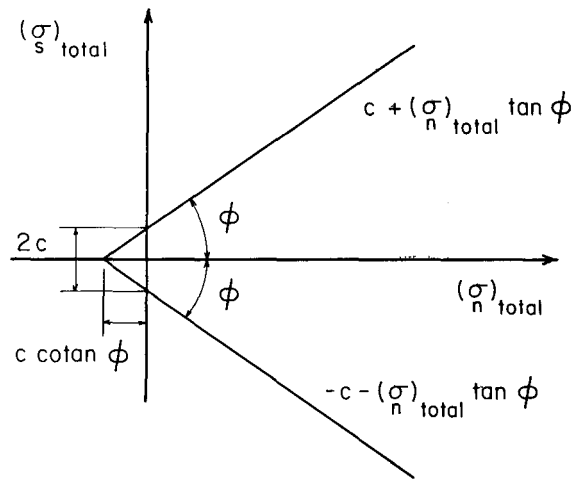

Fig. 3—Mohr–Coulomb envelope lines

Fulfilment of equations (7) for a cracked Mohr–Coulomb element can be accomplished during the course of iteration. If the trial normal stress $(\overset{i\,(k)}{\sigma})_{n\,\text{total}}$ is less than $-c$ cotan ϕ, we can use equations (7) to obtain the next approximations of the closure and ride at the i-th element. In general, however, under this approach the element will appear to oscillate between a cracked and an uncracked condition, and a satisfactory rate of convergence of the iteration process cannot be achieved. A better way of modelling a cracked element is to change its 'status' to that of a mined seam element. This guarantees that the total stresses across the element will be zero and prevents oscillation between two different conditions. It is essential, however, that one obtains a sufficiently accurate estimate of the normal stress before making the decision to change the status of the element. It has been found that twenty iterations are usually adequate for this purpose[9].

'Complete Closure' Restriction

In certain cases, a Mohr–Coulomb element that has cracked open at one stage of mining may close up again

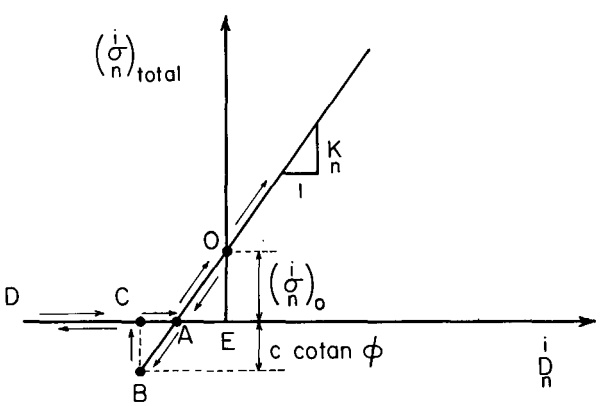

Fig. 4—Re-closure of a cracked Mohr–Coulomb element

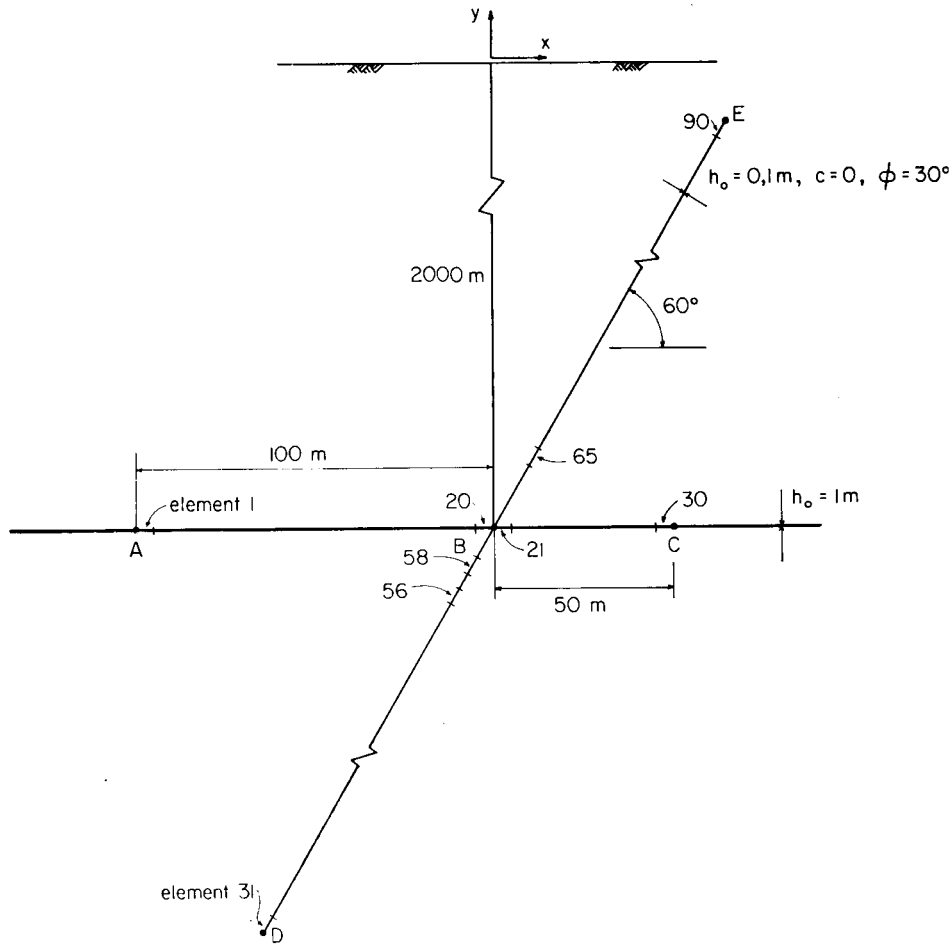

Fig. 5—Geometry in the example

at a later stage. This occurrence can be handled in the same way as a complete closure condition for a mined seam element. An important difference, however, is that the complete closure limit for a cracked Mohr–Coulomb element is *not* equal to the thickness of the element. This can be seen from Fig. 4, which shows a total normal stress–closure curve for a Mohr–Coulomb element.

Point 0 in Fig. 4 represents the conditions at the i-th Mohr–Coulomb element before any mining takes place; the initial normal stress is $\underset{n}{(\sigma)}_0^i$ and the initial closure is zero. The element cracks when the normal stress is equal to $-c$ cotan ϕ, indicated by point B in the figure. At this stage, the element will follow path CD if it continues to open. If the element subsequently closes up again, it will follow path DCAO, as shown in the figure. A 'complete closure' condition is therefore reached at point A. The length of line AE is $\underset{n}{(\sigma)}_0^i/\underset{n}{K}$, and it follows that a complete closure condition must be enforced whenever $\underset{n}{D}^i \geqslant -\underset{n}{(\sigma)}_0^i/\underset{n}{K}$.

Example of the Procedures

As an illustration of the procedures outlined above, we shall consider a particular example involving the mining of a flat-lying reef that intersects a fault. The geometry and material properties assumed for this example are hypothetical, but the main features of the problem are often encountered in practice. The numerical results discussed below were obtained using a computer program called MINAP, which is listed and documented elsewhere[10].

The geometry for the problem is shown in Fig. 5. The reef, which we assume is initially unmined, is at a depth of 2000 m and is intersected by a fault that dips at an angle of 60°. We shall assume that the stoping height in the reef plane is $h_0=1$ m, and that the cohesion and angle of friction of the fault are 0 and 30°, respectively. Further, we shall take the modulus of elasticity and Poisson's ratio of the host rock as $E=0{,}7\times10^5$ MPa and $\nu=0{,}2$. The elastic moduli for the reef are $E_{\text{reef}}=0{,}7\times10^5$ MPa and $G_{\text{reef}}=0{,}292\times10^5$ MPa (i.e., $\nu_{\text{reef}}=0{,}2$), and those for the fault are $E_{\text{fault}}=0{,}35\times10^5$ MPa and $G_{\text{fault}}=0{,}145\times10^5$ MPa. The fault thickness is 0,1 m. Finally, we shall suppose that the primitive stresses are uniform along any plane parallel to the reef, but that they vary linearly with depth. If the unit weight of the rock is 0,027 MN/m³, the primitive stresses are $(\sigma_{yy})_0=-0{,}027y$ MPa, $(\sigma_{xx})_0=k(\sigma_{yy})_0$ and $(\sigma_{xy})_0=0$, where $-y$ is the depth beneath the surface in metres

(see Fig. 5) and k is a constant. In order to examine the effects of the primitive stress state for this example, we shall treat constant k as a parameter with the values $\frac{1}{2}$, 1, and 2.

The purpose of the example is to examine the behaviour of the fault as a 150 m portion of the reef is mined, the portion labelled AC in Fig. 5. In solving the problem, reef AC was divided into 30 'seam' elements, each 5 m wide. The numbering scheme used to identify the separate elements is shown in the figure. The intersection of the reef and the fault plane, point B in Fig. 5, occurs just between elements 20 and 21. The two sections of the fault plane, labelled DB and BE, are each 150 m long. These sections were each divided into 30 Mohr–Coulomb elements 5 m wide. Element numbers 31 to 60 lie on the section of the fault beneath the reef, and elements 61 to 90 lie on the section above it.

Mohr Diagrams

A convenient way of representing the changing stress conditions on an element of the fault is shown in Fig. 6. This figure, called a Mohr diagram, shows the total shear stress as a function of the total normal stress for a particular Mohr–Coulomb element (element 65 in Fig. 5) if it is assumed that $(\sigma_{xx})_0=(\sigma_{yy})_0$, i.e., $k=1$. The circled numbers in the figure refer to the separate steps used to mine out portion AC of the reef, as indicated in Fig. 5. The two inclined straight lines in Fig. 6 represent the Mohr–Coulomb envelope for the case that the cohesion and angle of friction of the fault are $c=0$ and $\phi=30^\circ$, cf. Fig. 3. Because the stress conditions on element 65 always plot within the envelope for this case, we can conclude that the element does not experience any slip during the course of mining.

The situation is different, however, for certain other elements along the fault. A Mohr diagram for element number 56 is shown in Fig. 7. This element, like element 58, first undergoes slip at mining step 19, the step just before the one that 'breaks through' to the fault. As the excavation passes through the fault, element 56 'unloads' from the lower envelope line and eventually hits the upper one. The behaviour of element 57 is different in the sense that this element unloads directly from one envelope line to the other, eventually cracking open at the final mining step.

Similar diagrams could be plotted for the rest of the elements along the fault, but these are not sufficiently different from the ones already given to warrant separate consideration. It is instructive, however, to examine how the stresses transmitted across the fault are affected by the occurrence of yielding. We can do this by comparing the results above with those obtained from another simulation of the same problem in which slip is not allowed to occur. This comparison is made in Figs. 8 and 9 for elements 56 and 65, respectively. The circled numbers with primes indicate the mining step numbers for the case when the fault elements are not subject to the Mohr–Coulomb slip condition. The curves corresponding to the circled numbers without primes are the same as the ones given in Figs. 7 and 6. The results for the two cases are the same up to mining step 19, when slip first takes place under the conditions assumed for the case considered previously. At subsequent mining steps, however, the stress conditions on the fault elements are quite different for the two problems. On this basis, it appears that the capability of modelling slip along a fault is vital if one wishes to obtain a realistic estimate of the displacements and stresses induced by mining in faulted ground.

The foregoing results were obtained under the assumption that the horizontal primitive stress $(\sigma_{xx})_0$ is equal to the vertical primitive stress $(\sigma_{yy})_0$, i.e., $(\sigma_{xx})_0=k(\sigma_{yy})_0$ where $k=1$. Mohr diagrams for elements 56 and 65 are given in Figs 10 and 11, respectively, when $k=\frac{1}{2}$ and $k=2$. The results found previously for the case when $k=1$ are also plotted on these diagrams to aid in making comparisons. It can be seen that the three separate curves for the two elements initially have the same shape, but that they originate at different locations in the Mohr diagrams. Before any yielding has occurred, the shapes of the curves are controlled by the elastic induced stresses along the fault. These induced stresses, in turn, depend upon the primitive normal (and shear) stress acting on the reef plane, i.e., $(\sigma_{yy})_0$. The value of $(\sigma_{yy})_0$ on the reef plane is the same in all cases, $(\sigma_{yy})_0=$ 54 MPa, which explains why the curves shown in Figs. 10 and 11 initially have the same shape. These curves originate at different locations in the Mohr diagrams because the primitive stresses along the fault depend upon the value of the parameter k. It appears that the case $k=\frac{1}{2}$ is the most 'critical' of the three different cases considered, because the initial stress conditions along the fault lie fairly close to one branch of the Mohr–Coulomb envelope. Element 56, for example, undergoes slip at mining step number 14 and cracks open at step 19, which is just before the excavation intersects the fault. Element 65 experiences slip for $k=\frac{1}{2}$, but not for $k=1$ or $k=2$.

Energy Release Rates

Mohr diagrams are useful for examining how the mining of a reef affects the stress conditions along a fault, but these diagrams relate to individual elements and do not give an appreciation of how the occurrence of slip on any part of the fault may affect mining operations. The energy release rate due to mining does give such an appreciation, because it essentially 'integrates' the effects of all the elements and hence automatically incorporates the behaviour of the entire fault.

Energy release rates for the problem at hand are shown in Fig. 12 for the primitive stress state represented by parameter $k=1$. In the absence of any slip along the fault, this curve, like those for $k=\frac{1}{2}$ and $k=2$, would approximate a straight line, shown by a broken line in the figure*. The effects of slip along the fault can therefore easily be identified in the figure. It appears that, for all three values of k, the energy release rate increases abruptly as the excavation intersects the fault (mining step 20), falls off to a value less than the value that would occur in the absence of slip, and then in-

*In the absence of slip, the energy release rate is controlled by the primitive normal stress on the reef, which in this example does not depend on parameter k.

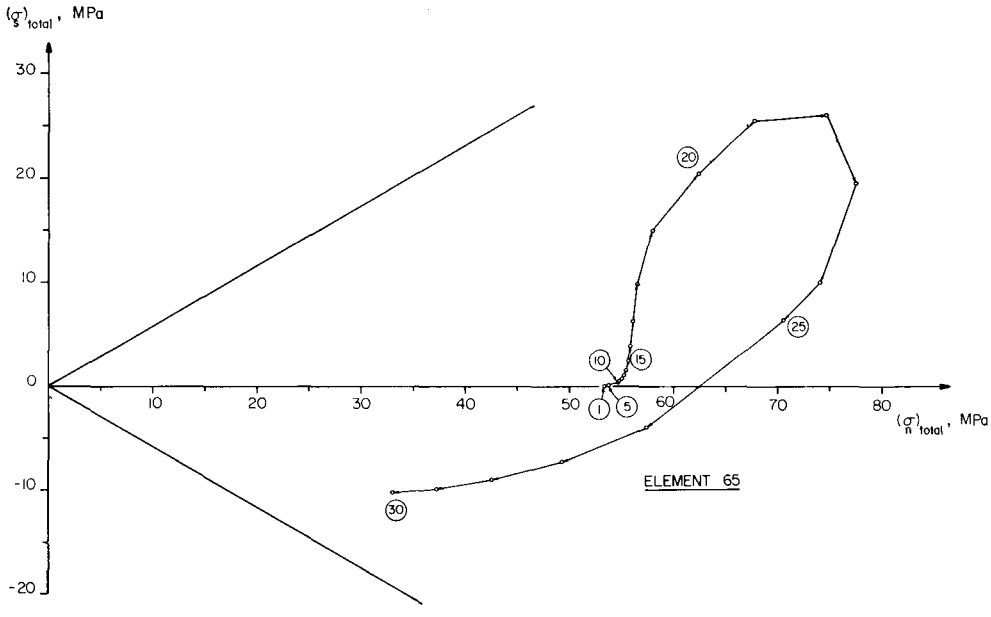

Fig. 6—Stress conditions for element 65 as a function of mining step number (k=1)

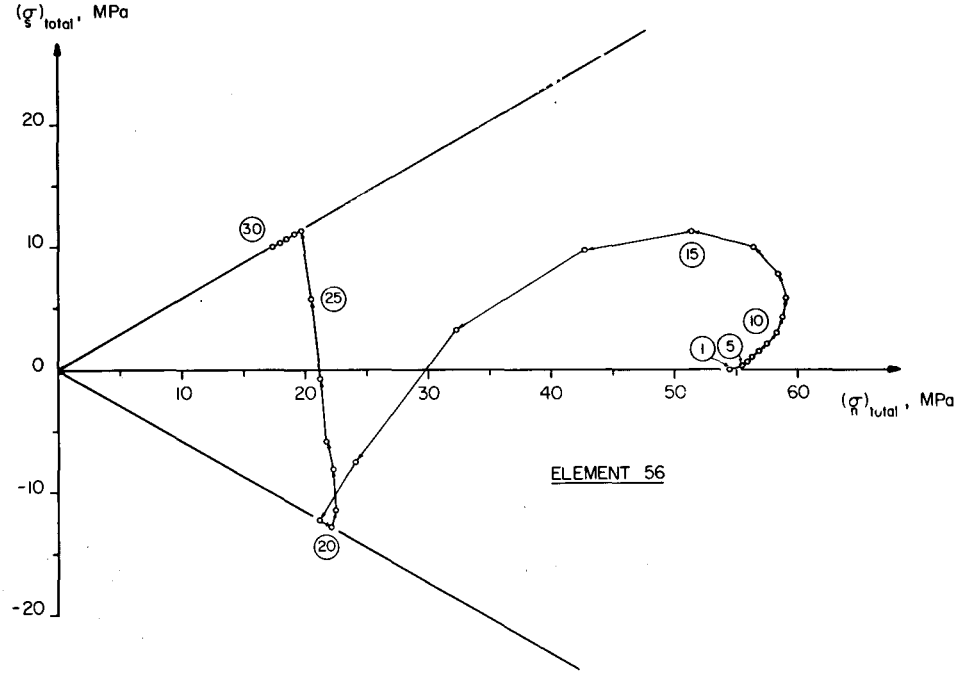

Fig. 7—Stress conditions for element 56 as a function of mining step number (k=1)

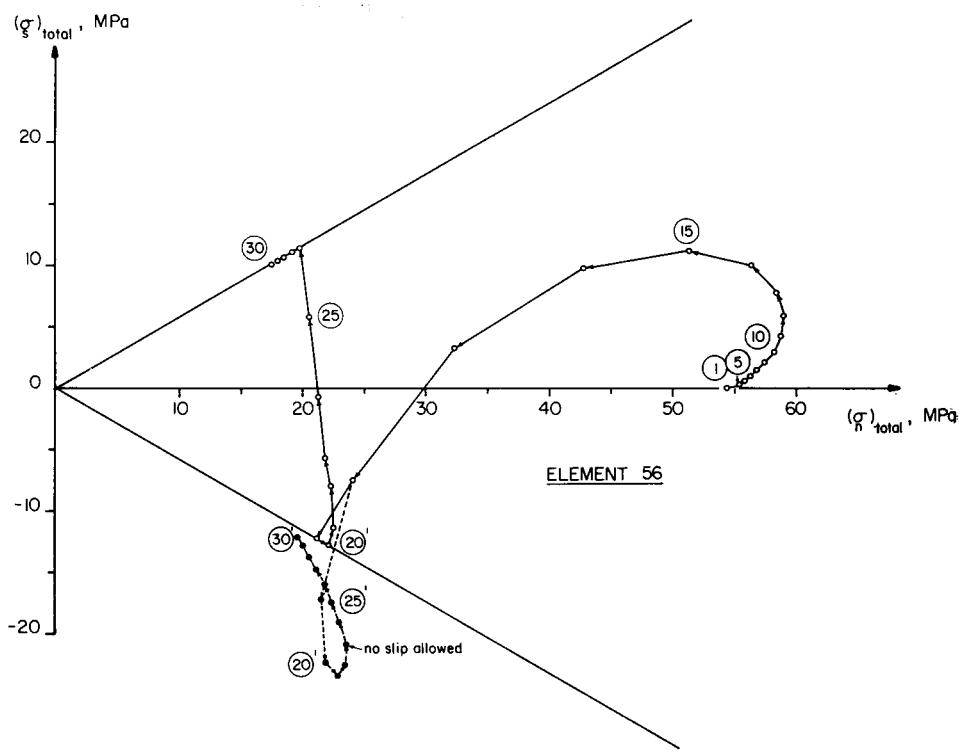

Fig. 8—Effects of fault slip on stress conditions for element 56 (k=1)

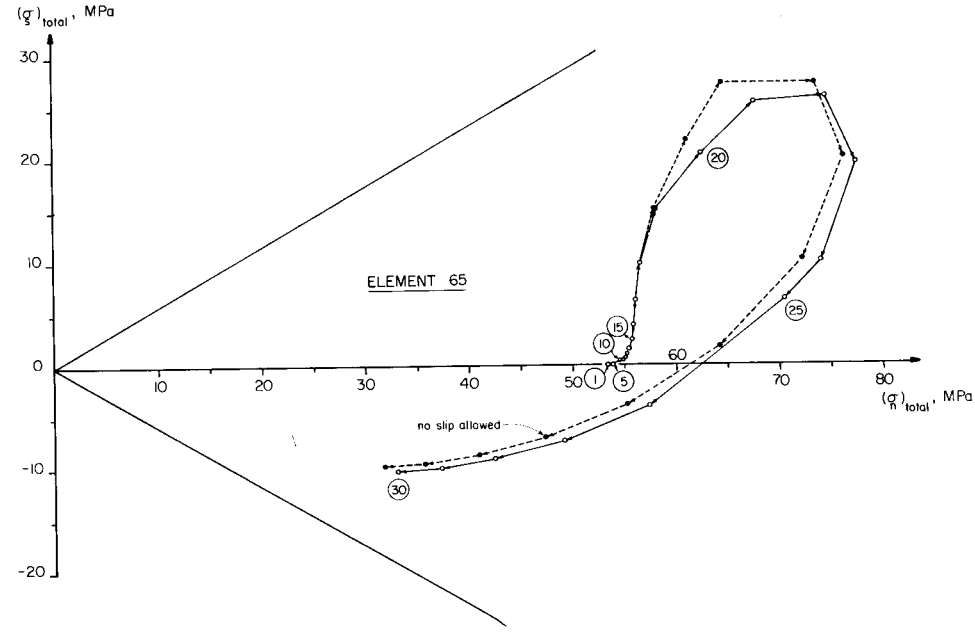

Fig. 9—Effects of fault slip on stress conditions for element 65 (k=1)

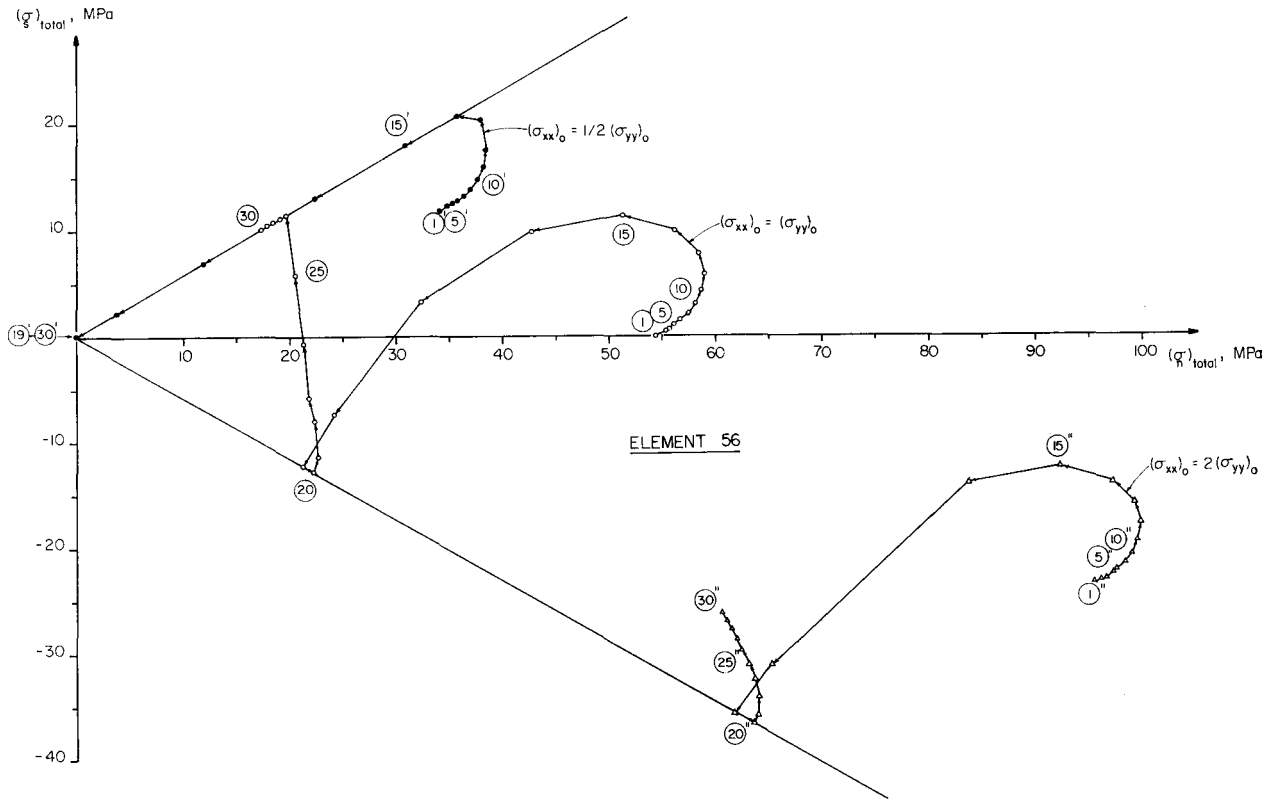

Fig. 10—Influence of initial stress conditions for element 56

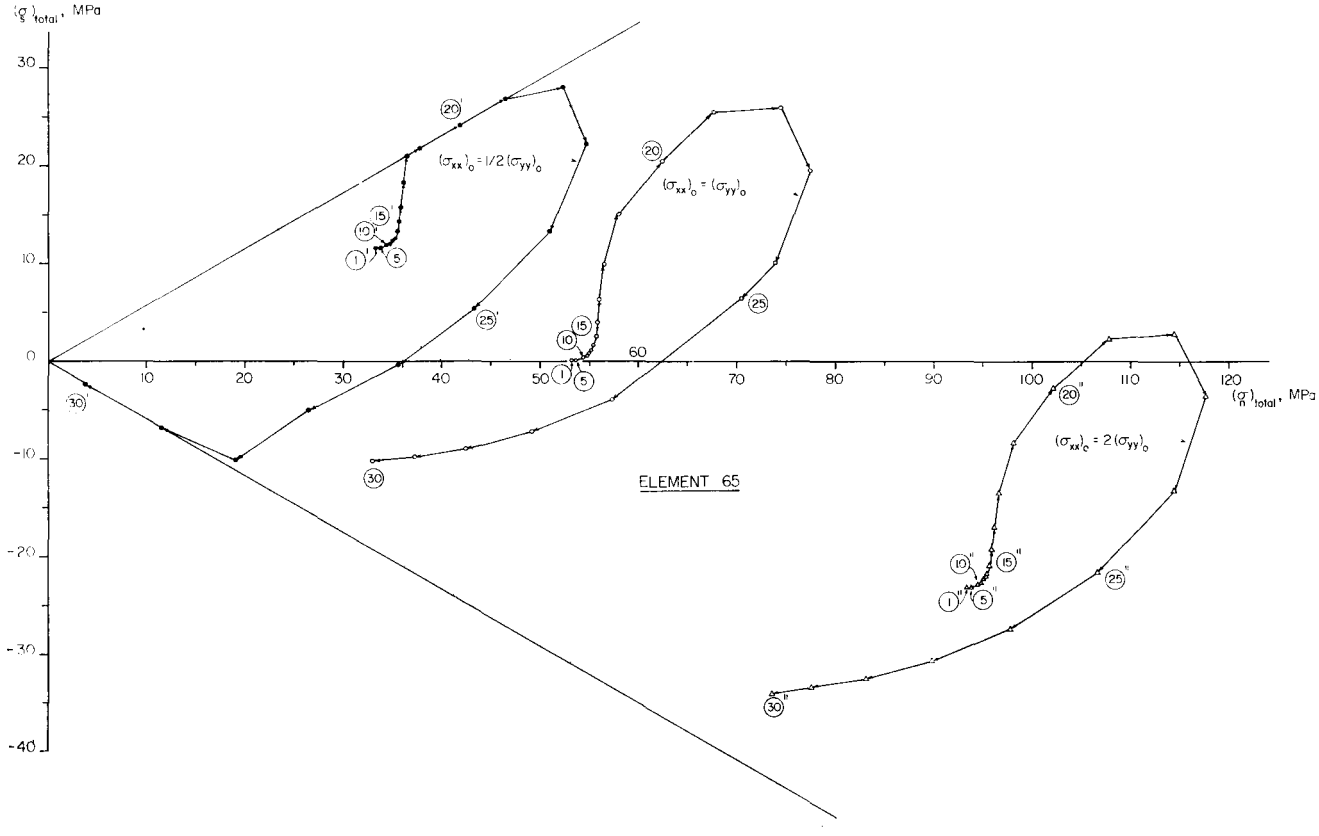

Fig. 11—Influence of initial stress conditions for element 65

creases at an increasing rate to rejoin the reference curve. Slip along the fault thus leads to a localized perturbation of the energy release rate due to mining. Another way of showing this is given in Fig. 13. This figure gives the change in the energy release rate with respect to the reference case in which no slip occurs along the fault. The results for $(\sigma_{xx})_0=2(\sigma_{yy})_0$ are nearly the same as those for $(\sigma_{xx})_0=(\sigma_{yy})_0$ and for clarity are not plotted. When $(\sigma_{xx})_0=\frac{1}{2}(\sigma_{yy})_0$ (i.e., when $k=\frac{1}{2}$), the energy release rate decreases slightly before the excavation intersects the fault, but the reduction is small and cannot be regarded as significant. A more

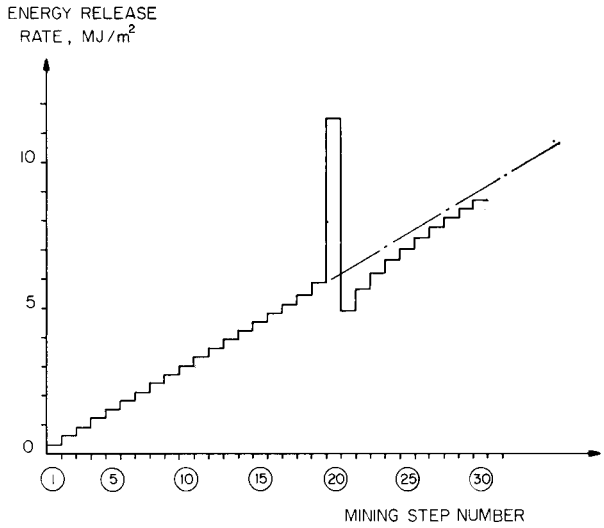

Fig. 12—Energy release rates as functions of mining step number for $k=1$

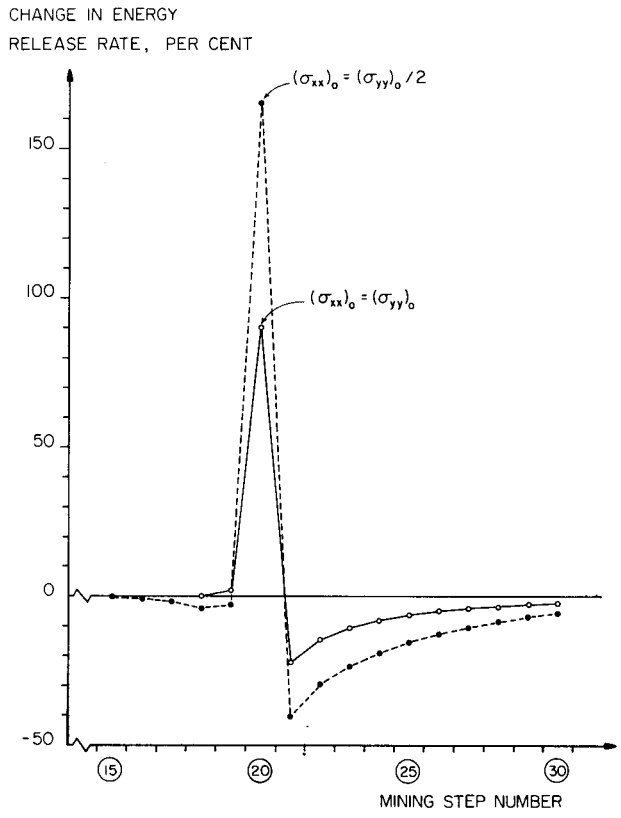

Fig. 13—Changes in energy release rate due to the occurrence of fault slip

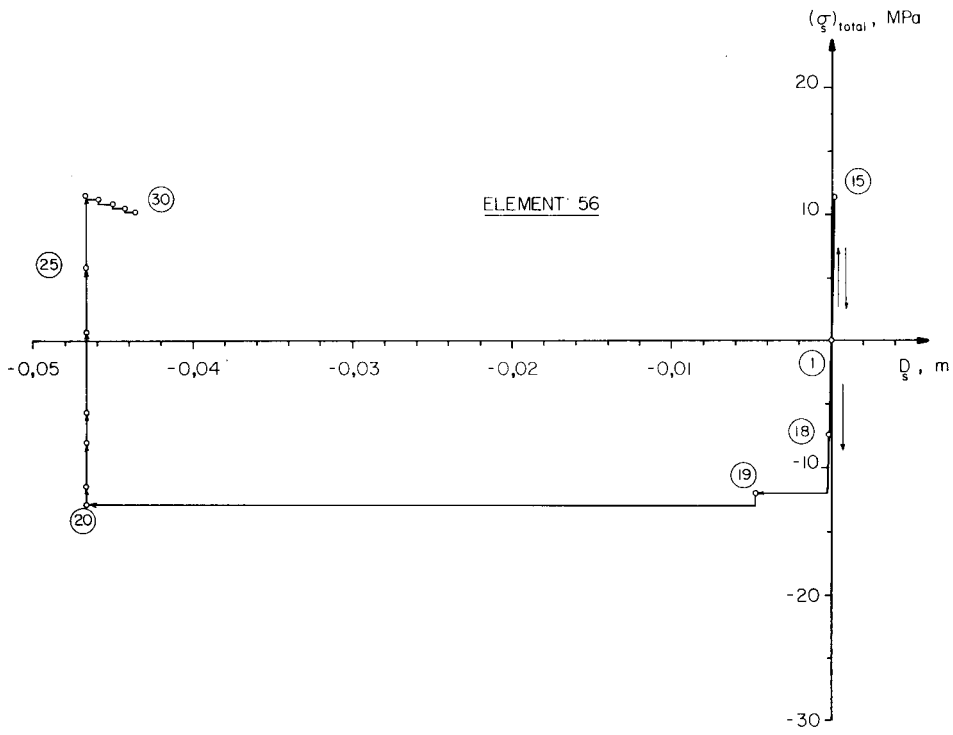

Fig. 14—Total shear stress–ride curves for element 56 ($k=1$)

interesting observation is that, as the excavation intersects the fault and then passes through it, a large increase in the energy release rate is followed by a correspondingly large decrease in this rate.

Energy Dissipation along the Fault

Another way of gaining insight into the effects of a fault on mining operations is to consider the amount of energy dissipated by slip along the fault. The energy dissipated by a particular element of the fault during slip is given by the product of the shear force and the amount of slip that occurs under it. The shear force (per unit length along the strike of the fault) is equal to the shear stress, $(\sigma)_{s\ total}$, times the width of the element, which in the present example is 5 m. We can find the amounts of slip that occur at a particular mining step by plotting curves of shear stress versus ride, such as shown in Figs. 14 and 15 for elements 56 and 65. The results for element 56 (Fig. 14) are for the case that $k=1$, and those for element 65 (Fig. 15) are for $k=\frac{1}{2}$. These figures should be examined with reference to the appropriate Mohr diagram given in Figs. 10 and 11. The amounts of slip and the occurrence of reversals in the directions of slip are depicted clearly in Figs. 14 and 15.

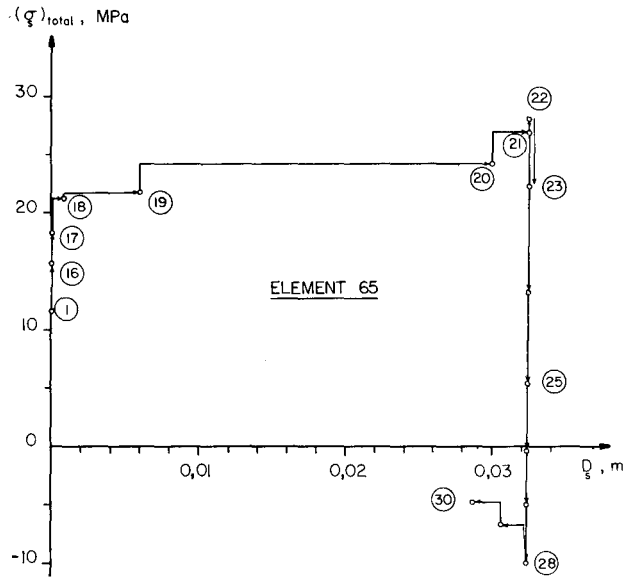

Fig. 15—Total shear stress–ride curves for element 65 ($k=\frac{1}{2}$)

Considering all of the elements along the fault, we can compute the energy dissipation (if any) at each mining step. The results of this computation are summarized in Fig. 16 for the three primitive stress states represented by $k=\frac{1}{2}$, 1, and 2. This figure shows the *cumulative* energy dissipation for a length L along the strike of the fault as a function of the mining step number. The largest amounts of energy dissipation occur at mining step 20, i.e., just as the excavation intersects the fault. Dissipation of energy appears to be a somewhat 'smoother' process for the case when $k=\frac{1}{2}$ than it is for $k=1$ or 2. In all cases, however, it must be concluded

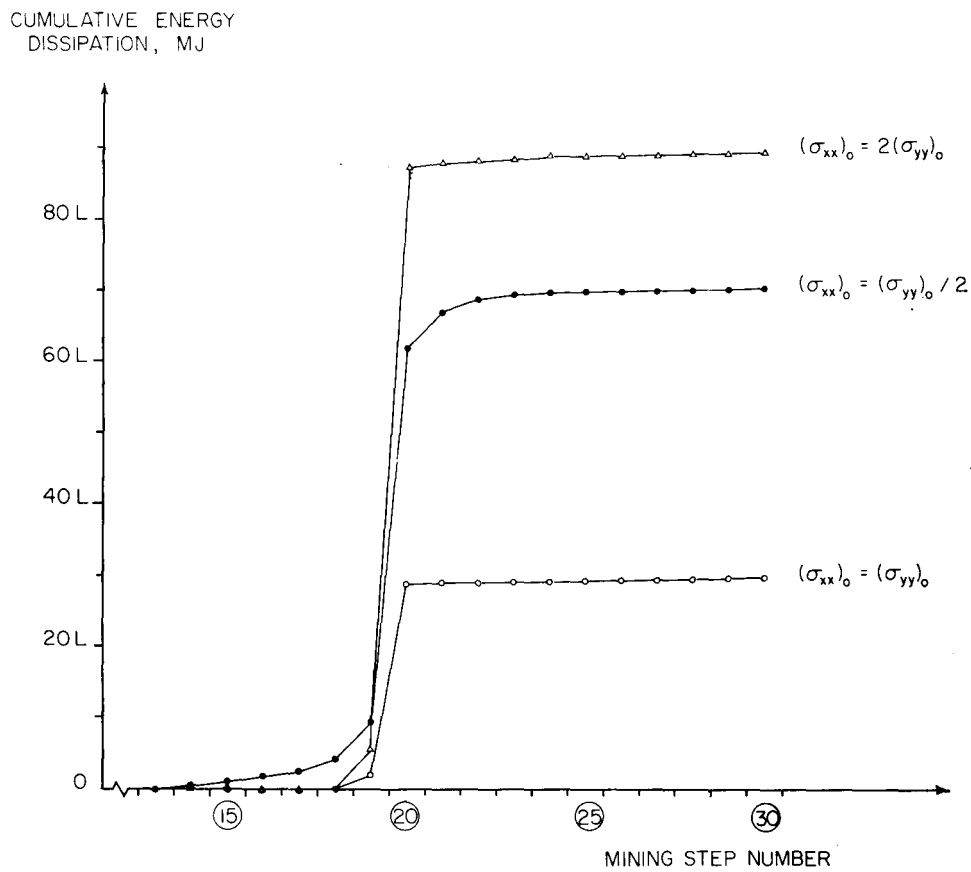

Fig. 16—Cumulative energy dissipation along fault as a function of mining step number

that the bulk of the energy dissipation occurs rather abruptly, with little advance notice.

Conclusion

The numerical procedures described in this paper can be applied to a variety of practical mining problems, even though the two-dimensional character of these procedures naturally imposes a limitation on the kinds of problems that can be modelled directly. For example, it will seldom happen that a problem involving a fault or a system of faults can be represented accurately in two dimensions. Even if the mining geometry is suitable for a two-dimensional analysis, a fault will not normally intersect the reef plane along a line perpendicular to the direction of face advance, making the problem fundamentally three-dimensional. Nonetheless, the capability of modelling the behaviour of joints and faults in a realistic way makes the two-dimensional displacement discontinuity method useful in a study of general design problems. Consideration of examples similar to that presented in this paper should help to establish guidelines for the planning of excavation layouts in faulted ground.

Acknowledgements

The numerical procedures described in this paper are based upon research supported by the U.S. National Science Foundation, Research Applied to National Needs Program under Grant GI-37923 (1973-76) and by the Office of Waste Isolation, Union Carbide Corporation, Nuclear Division under Subcontract No. 7118 (1976-present).

Parts of this paper were written while the author was a Visiting Lecturer in the Department of Applied Mathematics at the University of the Witwatersrand, Johannesburg, during 1976-77. He is grateful to the University Computer Centre for allowing him unrestricted use of their computer facilities during his stay in South Africa.

References

1. Salamon, M. D. G. Elastic analysis of displacements and stresses induced by mining of seam or reef deposits, Part I. *J. S. Afr. Inst. Min. Metall.*, vol. 64, no. 4. 1963. pp. 128-149.
2. Salamon, M. D. G. Elastic analysis of displacements and stresses induced by mining of seam or reef deposits, Part II. *J. S. Afr. Inst. Min. Metall.*, vol. 64, no. 6. 1964. pp. 197-218.
3. Salamon, M. D. G. Elastic analysis of displacements and stresses induced by mining of seam or reef deposits, Part IV. *J. S. Afr. Inst. Min. Metall.*, vol. 65, no. 5. 1964. pp. 319-338.
4. Salamon, M. D. G. Rock mechanics of underground excavations. *Proceedings of the Third Congress of the International Society for Rock Mechanics*, vol. I b, 1974. pp. 951-1099.
5. Plewman, R. P., Deist, F. H., and Ortlepp, W. D. The development and application of a digital computer method for the solution of strata control problems. *J. S. Afr. Inst. Min. Metall.*, vol. 70, no. 2. 1969. pp. 214-235.
6. Moris, J. P. E. SHAMIP: A computer program for elastic analysis of large size, tabular, mono-planar, shallow, hard orebodies. Johannesburg, Chamber of Mines of South Africa, *Research Report* no. 51/75. 1975. 221 pp.
7. Starfield, A. M., and Fairhurst, C. How high-speed computers advance design of practical mine pillar systems. *Engng Min. J.*, vol. 169, no. 5. 1968. pp. 78-84.
8. Starfield, A. M., and Crouch, S. L. Elastic analysis of single seam extraction. *New Horizons in Rock Mechanics* (ed. H. R. Hardy, Jr and R. Stefanko). New York, American Society of Civil Engineers, 1973. pp. 421-439.
9. Crouch, S. L. Solution of plane elasticity problems by the displacement discontinuity method. Part I. Infinite body solution, Part II. Semi-infinite body solution. *Int. J. num. Meth. Engng*, vol. 10. 1976. pp. 301-343.
10. Crouch, S. L. Analysis of stresses and displacements around underground excavations: an application of the displacement discontinuity method. Minneapolis, University of Minnesota, *Geomechanics Report to the National Science Foundation*. 1976. 268 pp.

Light metals

The 7th International Light Metal Congress will take place from 22nd to 26th June, 1981. The organizers of these meetings, which take place traditionally every few years, are the Austrian Metals Industry Association, the Austrian aluminium industry, and the Mining University of Leoben, in collaboration with Aluminium-Zentrale, Düsseldorf. As on the last occasion in 1975, the meetings will be held in Leoben (Styria) and Vienna. The programme is devoted mainly to aluminium.

Enquiries should be directed to Sekr., 7 Internationale Leichtmetalltagung, c/o Montanauniversität, A-8700 Leoben, Österreich.

Conference on fracture

The Fifth International Conference on Fracture is to be held at Cannes, France, from 29th March to 3rd April, 1981.

The following main topics will feature on the programme:

1. Practical applications of fracture mechanics
2. Crack tip singularity computations
3. Physical fracture processes; structural aspects
4. Elastoplastic fracture mechanics
5. Fatigue
6. Influence of environment on fracture toughness
7. Testing techniques.

Further information is obtainable from the General Secretary, Jacques POIRIER-CEA-DMECN, BPn° 2, 91190-GIF-SUR-YVETTE-FRANCE.

Planning and the environment

Little attention has been given in the past in South Africa in big development projects — roads, harbours, dams, mines — to the effects such schemes could have on the environment. The need to consider environmental aspects in the planning and development of projects has been a source of considerable conflict between developers and environmentalists, but the extreme views of both sides have been greatly softened in the course of the debate and the time has now come to resolve the dispute.

There is general agreement that environmental impact assessment (EIA) should form part of the planning for all major development projects. A symposium on 'Shaping Our Environment' is being held to help launch EIA in South Africa and is being organized by

- the Council for the Habitat, representing the concerned public and private environmental bodies in South Africa;
- EPPIC (Environmental Planning Professions Interdisciplinary Committee), representing the planning professions (architects, landscape architects, town and regional planners, land surveyors, civil, mining and electrical engineers);
- the Department of Planning and the Environment, representing Government;
- the CSIR, which, through its National Programme for Environmental Sciences, represents a broad spectrum of scientists and scientific and engineering disciplines;
- the CSIR Conference Division, which is providing the secretarial services.

The proposed aims are as follows:

- to emphasize the value of Environmental Impact Assessment (EIA) as an aid to the management of environmental change in South Africa resulting from development;
- to examine the matrix and other EIA methods currently in use or proposed and their application to:
  procedures for preliminary assessments
  proposed methods and guidelines for professional EIA studies, and
  the assessment of more extensive and complex environmental changes;
- to create an awareness of the need for long-term monitoring as a follow-up to EIA studies;
- to consider the necessary professional self-discipline, legal framework and acceptable administrative mechanisms for the effective implementation of EIA in South Africa.

The symposium is to be held in Pretoria on 1st and 2nd August, 1979. Enquiries should be directed to The Symposium Secretariat S. 190, Conference Division, C S I R, P.O. Box 395, Pretoria 0001. (Telephone 012 74-9111 X 2070 or 2800).

Natal Building Society Visiting Fellowship

The Natal Building Society Visiting Fellowship has been established to finance visits by eminent authorities from overseas to visit South Africa for the purpose of seminars, discussions, consultation, and possible active participation in scientific, technological, and development projects of importance to the building industry. It is financed by the Natal Building Society and is operated jointly by that body, the Building Industries Federation (South Africa), the Institute of S.A. Architects, the Association of South African Quantity Surveyors, and the National Building Research Institute of the CSIR.

The Fellowship scheme functions as follows:

(a) Nominations for suitable candidates for the Fellowship are invited annually by announcements in technical and professional journals serving the building industry. These are then considered by the Natal Building Society Fellowship Awards Committee, which will select the person who it feels could make the most useful contribution to local knowledge.

(b) The persons selected will be authorities in areas of activity of topical importance to the building industry.

(c) An invitation is then sent to the selected individual to visit South Africa during the following year.

(d) The duration of the visit is nominally one month, but it could also be for a slightly shorter or longer period.

(e) The visits may coincide with congresses or other appropriate functions being arranged in that particular year, and arrangements will be made for the Fellow to take a leading part in such functions and to give a limited number of lectures in a few of the main centres in South Africa.

(f) The Fellowship will cover
  (i) economy-class air travel for the Fellow from his normal place of residence to South Africa and return;
  (ii) costs of travel in South Africa to various centres;
  (iii) a subsistence allowance of R30 a day to cover his hotel and incidental expenses for the period that he spends in South Africa.

(g) During the tenure of the Fellowship, the Fellow will meet leaders of the building society movement, the building industry, the professions, the public sector, and the universities to discuss his impressions during the visit and matters in his field of expertise.

(h) Requests for nomination forms should be addressed to The Head, University Research Division, P.O. Box 395, Pretoria, 0001. Formal nominations, channelled through and endorsed by a South African university or one of the following organizations BIFSA, ISAA, ASAQS or NBRI, should be received on or before 30th March, 1979.